OPEN ACCESS Freely available online

PLoS one

Blockade of Persistent Sodium Currents Contributes to the Riluzole-Induced Inhibition of Spontaneous Activity and Oscillations in Injured DRG Neurons

Rou-Gang Xie[1☯], Da-Wei Zheng[1☯], Jun-Ling Xing[1☯], Xu-Jie Zhang[1,2☯], Ying Song[1,4], Ya-Bin Xie[1], Fang Kuang[1], Hui Dong[3], Si-Wei You[1], Hui Xu[1]*, San-Jue Hu[1]*

1 Institute of Neuroscience, Xi Jing Hospital, The Fourth Military Medical University, Xi'an, People's Republic of China, **2** School of Stomatology, Xi Jing Hospital, The Fourth Military Medical University, Xi'an, People's Republic of China, **3** Department of Anaesthiology, Xi Jing Hospital, The Fourth Military Medical University, Xi'an, People's Republic of China, **4** Jiangsu Province Key Laboratory of Anesthesiology, Xuzhou Medical College, Xuzhou, People's Republic of China

Abstract

In addition to a fast activating and immediately inactivating inward sodium current, many types of excitable cells possess a noninactivating or slowly inactivating component: the persistent sodium current (I_{NaP}). The I_{NaP} is found in normal primary sensory neurons where it is mediated by tetrodotoxin-sensitive sodium channels. The dorsal root ganglion (DRG) is the gateway for ectopic impulses that originate in pathological pain signals from the periphery. However, the role of I_{NaP} in DRG neurons remains unclear, particularly in neuropathic pain states. Using *in vivo* recordings from single medium- and large-diameter fibers isolated from the compressed DRG in Sprague-Dawley rats, we show that local application of riluzole, which blocks the I_{NaP}, also inhibits the spontaneous activity of A-type DRG neurons in a dose-dependent manner. Significantly, riluzole also abolished subthreshold membrane potential oscillations (SMPOs), although DRG neurons still responded to intracellular current injection with a single full-sized spike. In addition, the I_{NaP} was enhanced in medium- and large-sized neurons of the compressed DRG, while bath-applied riluzole significantly inhibited the I_{NaP} without affecting the transient sodium current (I_{NaT}). Taken together, these results demonstrate for the first time that the I_{NaP} blocker riluzole selectively inhibits I_{NaP} and thereby blocks SMPOs and the ectopic spontaneous activity of injured A-type DRG neurons. This suggests that the I_{NaP} of DRG neurons is a potential target for treating neuropathic pain at the peripheral level.

Citation: Xie R-G, Zheng D-W, Xing J-L, Zhang X-J, Song Y, et al. (2011) Blockade of Persistent Sodium Currents Contributes to the Riluzole-Induced Inhibition of Spontaneous Activity and Oscillations in Injured DRG Neurons. PLoS ONE 6(4): e18681. doi:10.1371/journal.pone.0018681

Editor: Mark L. Baccei, University of Cincinnati, United States of America

Received October 27, 2010; **Accepted** March 11, 2011; **Published** April 25, 2011

Funding: This work was supported by the National Natural Science Foundation of China (Grant NO. 30870830 and 30600581). The funders had no role in study design, data collection and analysis, decision to publish, or preparation of the manuscript.

Competing Interests: The authors have declared that no competing interests exist.

* E-mail: sjhu@fmmu.edu.cn (SJH); xubz@fmmu.edu.cn (HX)

☯ These authors contributed equally to this work.

Introduction

Voltage-dependent sodium channels are responsible for the generation and conduction of action potentials in the membranes of excitable cells. In addition to a fast activating and immediately inactivating sodium current, the inward current of many types of excitable cells also has a non-inactivating or slowly inactivating component: the persistent sodium current (I_{NaP}). The I_{NaP} is present in neurons throughout the central nervous system, including those of the hippocampus, neocortex and cerebellum [1]; it has also been found in thalamic neurons [1,2], mesencephalic trigeminal sensory neurons [3], and hypoglossal motoneurons [4]. When present, I_{NaP} lowers the actviation threshold of most neurons by about 10 mV, and is blocked by a low level of tretrodotoxin (100 nM) [1,5,6]. Under physiological conditions, I_{NaP} is critical to neuronal excitability, the modulation of near-threshold membrane potentials, the amplification of synaptic currents, and the facilitation of repetitive firing [7,8,9,10]. There is evidence from a genetic model of amyotrophic lateral sclerosis and spinal cord injury that an increased persistent sodium current determines the hyperexcitability of central cortical neurons [11,12]. It also has been reported that I_{NaP} participates in epileptic firing in the central nervous system [5]. Among such cells as mesencephalic trigeminal sensory neurons and hippocampal neurons, I_{NaP} is considered to be one of the threshold currents modulating neuronal excitability under both physiological and pathological conditions.

Recently, a number of reports have focused on the effects of riluzole on I_{NaP} in central neurons [13,14,15,16,17], and have proposed riluzole as a relatively specific persistent sodium channel blocker [18,19]. Riluzole has been used clinically in the treatment of several neurological disorders, including amyotrophic lateral sclerosis [20] and epilepsy. However, the mechanisms underlying these clinical applications are far from clear.

The dorsal root ganglion (DRG) is the gateway for ectopic impulses originating in pathological pain signals from the periphery. The I_{NaP} has been found in normal primary sensory neurons where it is mediated by tetrodotoxin-sensitive sodium channels [21]. However, the role of I_{NaP} in DRG neurons is uncertain, particularly in neuropathic pain states. Our recent work has shown that in compressed DRG neurons, I_{NaP} is blocked by gabapentin and low doses of lidocaine, and that these analgesic

drugs suppress the submembrane potential oscillations of injured DRG neurons [22,23].

In the present study we demonstrate that behavioral changes in rats undergoing a chronic compression of the dorsal root ganglion (CCD) [24,25] are concurrent with a significant enhancement of I_{NaP}, along with its associated subthreshold membrane potential oscillations (SMPOs) and ectopic spotaneous activity (SA), in the correspondingly injured A-type DRG neurons. Local application of riluzole clearly inhibits I_{NaP} while suppressing SMPOs and SA, indicating a potential role for the I_{NaP} of injured DRG neurons in neuropathic pain states.

Materials and Methods

1. CCD animal model

Experiments were conducted on adult Sprague–Dawley rats (200–250 g) of both sexes. The animals were purchased from the Animal Center of the Fourth Military Medical University (FMMU) and were housed and handled according to the guidelines of the institutional and national Committees of Animal Use and Protection.

The animal model used in this study was established in our department as described previously [24,25]. In the present study, a stainless steel L-shaped rod (4 mm in length and 0.66 mm in diameter) was implanted in the intervertebral forman at L5 to chronically compress the DRG.

2. Behavioral testing

Mechanical paw withdrawal threshold. Paw withdrawal thresholds to mechanical stimulation were assessed using von Frey filaments (Stoelting Co, USA). Each animal was placed on a metal mesh floor in a plastic cage (20×25×15 cm). To test the tactile threshold required to evoke withdrawal of the stimulated paw, von Frey filaments (2–15.0 g) were applied perpendicularly in ascending order to the plantar part of the hind paw [26]. Withdrawal, flicking, or licking of the hind paw were all considered positive responses. Each filament was applied five times, with the overall response assessed as positive if three or more positive responses of the hind paw were obtained. The paw withdrawal threshold was determined by the lowest strength of stimulation. To avoid tissue damage, the cut off threshold was assigned at 15.0 g [27].

3. Electrophysiological recordings

3.1 Extracellular recording of DRG single fiber activities. Unit activities of single DRG A-fibers were recorded 3–8 days after the CCD surgery. Under sodium pentobabital anesthesia (40 mg/kg, i.p.), laminectomies were performed at the L1–L2 and L4–L5 levels separately, and two small pools were formed above the exposure regions. In the L4–L5 pool the stainless steel rod was removed. The spinal nerve was transected 7–10 mm distal to the DRG so that the discharge activities of the dorsal root fibers would originate primarily from the DRG region and not from peripheral sources. During recording the L4–L5 pool was filled with warm Krebs solution (35–37°C) containing (in mM): NaCl 150, KCl 5, $CaCl_2$ 2, $MgCl_2$ 1, D-glucose 10 and HEPES 10, with the pH adjusted to 7.4.

The L1–L2 pool was filled with warm paraffin oil (35–37°C). Under a microscope, a microfilament (20–50 μm in diameter) and presumably including up to a few nerve fibers was isolated from the dorsal root and cut off. The proximal end was placed on a fine platinum electrode (29 μm in diameter) for electrophysiological recording of DRG single fiber activities. The firing patterns of a single fiber were displayed on a memory oscilloscope (VC-11, Japan) and recorded via an A/D board to a computer hard drive and stored for offline analysis. Unit activities with identical wave forms were selected as single fiber activities [24,28].

Riluzole (Sigma, USA) was dissolved in dimethyl sulfoxide (DMSO) as a stock solution and kept frozen; it was diluted in ACSF before the experiments. Unit discharges were recorded in the presence and absence of riluzole or vehicle for at least another 3 min. The percentage changes in discharge rate were calculated as: (maximal discharge rate - baseline rate)/baseline rate×100%. The changes in single fiber firing rates were considered significant if the differences were 15% or greater [28].

3.2 Intracellular recording of SMPOs in DRG neurons. In order to examine the effects of riluzole on these oscillations, DRG neurons from CCD animals were intracellularly recorded *in vivo* using sharp electrodes. The compressed DRG was exposed under sodium pentobabital anesthesia (40 mg/kg, i.p.). A small pool was formed surrounding the CCD ganglion and filled with warm paraffin oil, as described above. Recording microelectrodes were pulled from borosilicate glass tubes using a microelectrode puller (P97, Sutter Instruments, USA). After being filled with 3 M potassium acetate the microelectrodes had a final resistance of 40–60 MΩ. DRG neurons were impaled under visual control by advancing the microelectrode at 4–8 μm steps, with application of a small capacitance buzz when necessary.

The conduction velocity was measured by delivering a brief electrical pulse to the sciatic nerve through a stimulus isolator. DRG neurons were categorized by their conduction velocities [29]. Only A-type neurons with conduction velocities of 15.0–35.1 m/s having stable resting membrane potentials below −50 mV and/or spontaneous activity were selected for further investigation. Recordings were terminated if the resting membrane potential dropped more than 10% below control values. Riluzole (80 μM) was locally applied after control recordings.

3.3 Whole-cell patch recording of sodium currents in DRG neurons. Three to eight days after the CCD surgery, the animals that showed the positive behavioral responses described above were selected for further electrophysioloical recordings. After these animals were anesthetized with sodium pentobarbital (50 mg/kg, i.p.), the compressed L5 DRGs were carefully removed from the vertebral column and placed in cold oxygenated ACSF. The ACSF contained (in mM): NaCl 125, KCl 2.5, NaH_2PO4 1.2, $MgCl_2$ 1.0, $CaCl_2$ 2.0, $NaHCO_3$ 25, and D-glucose 10. The connective tissue was gently removed under a microscope and the ganglia were digested with a mixture of 0.4 mg/ml trypsin (Sigma) and 1.0 mg/ml A-type collagenase (Sigma) for 40 min at 37°C while agitated by gentle bubbling with 95% O_2 and 5% CO_2. Finally, the ganglion was transferred into a holding chamber containing normal ACSF bubbled with 95% O_2 and 5% CO_2 at 26°C [23].

Recording electrodes had resistances of 4–8 MΩ after being filled with an internal solution. To measure membrane potentials and the effects of riluzole on the SMPOs of A-type DRG neurons, the internal solution contained (in mM): KCl 140, $MgCl_2$ 2, HEPES 10, Mg-ATP 2, with the pH adjusted to 7.4. To examine the effects of riluzole on sodium currents in A-type DRG neurons, recording electrodes were filled with an internal solution containing (in mM): CsCl 110, NaCl 5, $MgCl_2$ 3, $CaCl_2$ 1, EGTA 3 and HEPES 40, adjusted with Tris buffer to pH 7.4. The bath solution consisted of (in mM): NaCl 100, TEA-Cl (tetraethylammonium chloride) 40, KCl 3, $MgCl_2$ 1, $CaCl_2$ 1, D-glucose 10, HEPES 10, $BaCl_2$ 1, CsCl 1, 4-AP (4-aminopyridine) 2 and $CdCl_2$ 0.1, with the pH adjusted to 7.4 [30].

The ganglion was kept in the holding chamber for at least 1 hr before being transferred to the recording chamber. During

recording, the ganglion was kept submerged and perfused with warm (32°C) ACSF saturated with 95% O_2 and 5% CO_2. Individual neurons were visualized with a 40× water-immersion objective under a microscope (BX51WI; Olympus) equipped with infrared differential interference contrast optics. Whole-cell current and voltage recordings were carried out using a Multiclamp 700B amplifier (Molecular Devices, USA). The signals were digitized at 10 kHz by a 1320 A/D board (Molecular Devices, USA) and stored in a computer hard drive for offline analysis. P-clamp 9 software (Molecular Devices, USA) was used for data acquisition and analysis. Typically, a gigaohm seal was formed by a small negative pressure, and whole-cell recording was established by rupture of the cell membrane with further negative pressure or a buzz signal, or a combination of both. Membrane potential was held at −60 mV under voltage clamp. Neurons that showed resting membrane potentials below −50 mV along with overshooting action potentials were selected for further study. Recordings were terminated if the R_a increased or resting membrane potential dropped by 20% or more from control levels.

Sodium current amplitude was transformed into conductance using the Ohm's law in the form: $G = I/(V-E_{Na})$, where V is the test potential and E_{Na} is the Na^+ equilibrium potential calculated using the Nernst equation. Conductance was normalized, plotted against V and fitted with a Boltzmann function of the form: $G/G_{max} = 1/\{1+\exp[(V-V_{1/2})\times k^{-1}]\}$, where $V_{1/2}$ is the half-activation voltage and k is the slope factor.

4. Statistical analysis

All values were expressed as mean ± SEM. Statistical evaluations were performed using Statistical Product and Service Solutions (SPSS) software (paired t-test, non-paired t-test, repeated measure, and one-way AVOVA methods) with the significance criterion set at $P = 0.05$.

Results

1. Mechanical allodynia in CCD animals

During the behavioral test period which lasted for up to two weeks, all animals appeared to be gaining weight, which suggests that they were in good health. Animals were usually well groomed and exhibited no self-inflicted wounds. No abnormal gait or posture was observed in the control group. However, all tested rats post-CCD surgery developed varying degrees of gait and postural abnormality. They were often seen to lift the ipsilateral hindpaw from the ground and then hold it in a protected position next to the flank while standing or sitting. When the affected hindpaw was touching the ground, the animals often reduced the weight placed on it by leaning to the other side or by sitting on the opposite haunch. These behaviors appeared as early as one day after the CCD surgery, and all animals showed such behaviors within the first two weeks, as reported earlier [24,25]. No control or test animals exhibited any signs of autotomy or abnormal nail growth. However, the CCD rats used for subsequent electrophysiological recordings showed clear behavioral indications of allodynia, as reported previously [24,25].

As shown in Figure 1A, the thresholds for paw withdrawal in control animals were relatively stable (8.5±0.4 g, n = 6), while the values for the same tests on the contralateral side were slightly decreased (Fig. 1B), but not to a statistically significant extent (non-paired t-test, $P>0.05$). However, the thresholds for paw withdrawal on the ipsilateral side of the CCD animals were clearly reduced starting on the day after the CCD surgery (one-way AVOVA method, $P<0.05$). The reductions became statistically significant from day 5 on and remained low until the end of the tests (4.0±0.8 g, n = 4; non-paired t-test, $P<0.05$, Fig. 1A). These behavioral responses of the CCD animals are characteristic of mechanical allodynia. Similar results have been reported by our group [24] and by others [25].

2. Inhibitory effects of I_{NaP} blocker riluzole on the spontaneous activity of A-type fibers from compressed DRG neurons

A total of 53 spontaneously discharging A-type single fibers of the L5 DRG were recorded from 38 CCD ganglions in intact animals. CCD fibers/neurons can be classified into two classes based on the dynamic features of their spontaneous activities [28]. The periodic class is characterized by the interspike intervals that appear repeatedly at regular intervals, and 21 of 53 fibers (39.6%) fell into this category. Fibers in the non-periodic class have an irregular pattern of interspike intervals, and 32 of 53 fibers (60.4%) were included in this group.

Basal firing rates normally fluctuated from 0.6% to 14.2% of the average control value (6.4±0.5%, n = 53). Five minutes after local application of the I_{NaP} blocker riluzole (100 μM) to the DRG region, rates of spontaneous activity were reduced in all cases

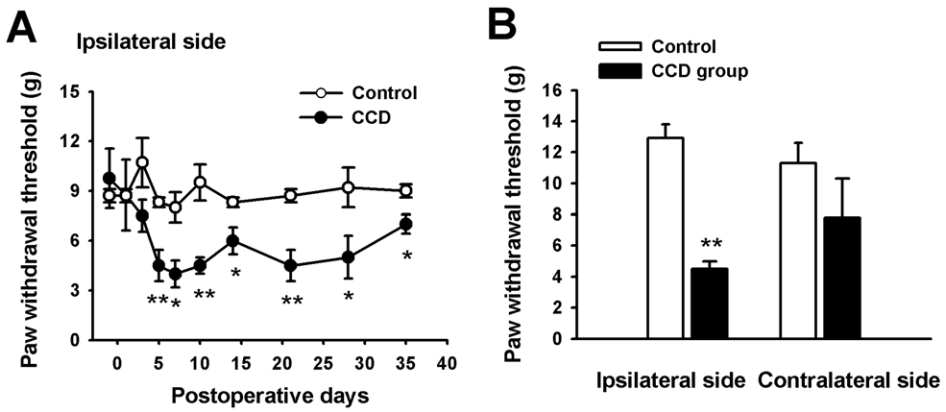

Figure 1. Mechanical allodynia in CCD rats. (A) Time course of changes in the withdrawl threshold of the ipsilateral hindpaw for control (n = 6, open circles) and CCD (n = 4, closed circles) rats. The mechanical threshold for withdrawl of the ipsilateral hindpaw was significantly lower in the chronically compressed rats (* $P<0.05$ or ** $P<0.01$ compared with the average for the ipsilateral hindpaw of the control group). (B) Average ipsilateral and contralateral paw withdrawl thresholds for the control and CCD groups on the postoperative 5 days.
doi:10.1371/journal.pone.0018681.g001

(n = 6). Figure 2A shows one such recording, in which firings were reversibly abolished after the riluzole application. The results of similar recordings can be summarized as showing that the spontaneous activity of A-type CCD fibers is suppressed by riluzole in a dose-dependent manner (n = 6, Fig. 2B). Again, the riluzole-mediated inhibition of the spontaneous activity in A-type CCD fibers was shown to be reversible in most cases, as the spontaneous activity resumed in 78.6% (22/28) of the fibers within 20 min after washout (Fig. 2A). In the presence of 0.1% DMSO, the discharge rate of A-type fibers from compressed DRG neurons was 19.9±2.9 Hz (n = 4), which is not significantly different from the discharge rate of A-type fibers in the absence of the vehicle (paired t-test, P>0.05).

3. Inhibitory effects of riluzole on SMPOs in compressed A-type DRG neurons

3.1 Inhibitory effects of riluzole on spontaneous SMPOs at the resting membrane potential. The SMPOs observed in DRG neurons of CCD animals can be considered a useful electrophysiological indication of neuronal injury. To examine whether riluzole affects SMPOs and would thereby block such downstream effects, DRG neurons in CCD animals were recorded *in vivo* using sharp electrodes. Upon penetration, most of these DRG neurons were silent and had a relatively stable membrane potential (−61.3±0.9 mV, n = 30), but some (7/63, 11.1%) displayed sinusoidal SMPOs (78.2±3.4 Hz, n = 12) and spontaneous activity at the resting membrane potential. After a 5 min period of baseline recording from 4 of such neurons, riluzole (80 μM) was locally applied onto the DRG. It was found that the resting membrane potential remained stable in all of these cells, but that the frequency of the spontaneous activity gradually decreased and finally disappeared in about 60 s. The SMPOs showed similar changes, decreasing in amplitude and then disappearing. The inhibition of riluzole on spontaneous activity and SMPOs was largely recovered following washout in all the tested neurons (Fig. 3A).

3.2 Inhibitory effects of riluzole on the spontaneous activity *in vitro*. Few if any DRG neurons recorded using whole-cell patch-clamp methods displayed spontaneous activity following the compression of the DRG. The effects of riluzole were examined in these neurons by the bath application of the drug (10 μM) to three DRG neurons *in vitro*, after which the spontaneous activity slowed down and eventually was eliminated (Fig. 3B).

3.3 Inhibitory effects of riluzole on SMPOs at different levels of depolarization. Using whole-cell patch-clamp methods, about a third of the recorded DRG cells (10/28, 35.7%) displayed high frequency sinusoidal SMPOs and repetitive discharges during the injection of 800 ms depolarizing current pulses. The effects of riluzole were examined in five of these neurons by the bath application of the drug (10 μM). It was found that the SMPOs were eliminated and that the repetitive firing slowed down and eventually stopped 3 min after the drug

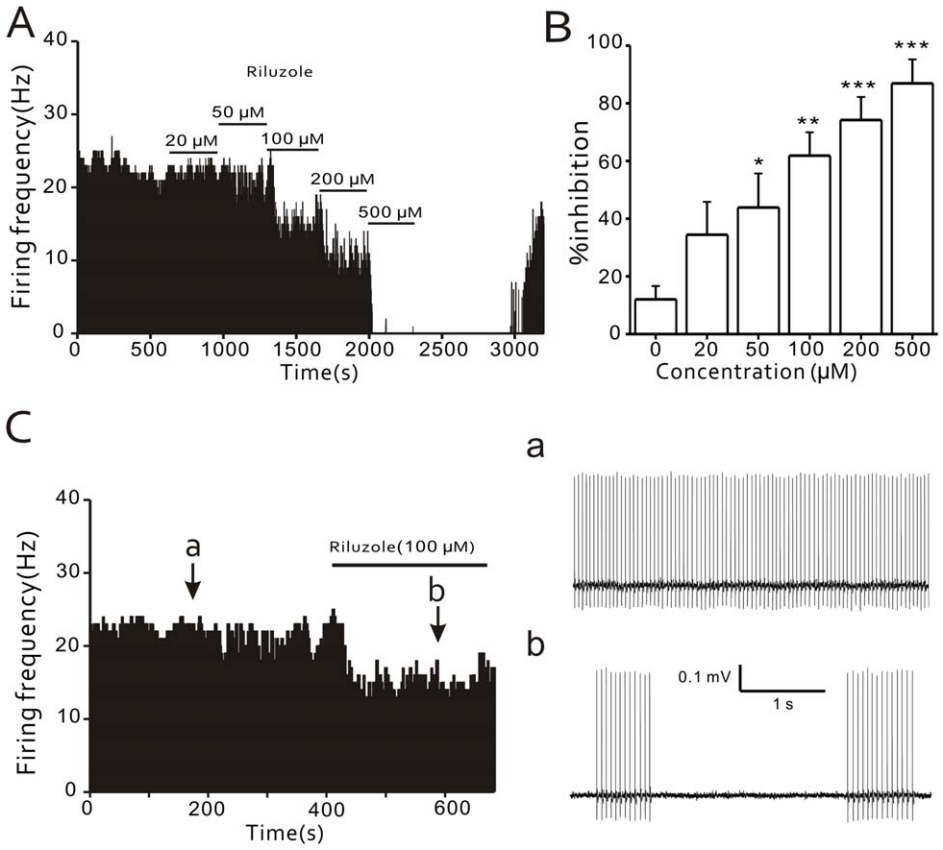

Figure 2. Effects of riluzole on the spontaneous activity of A-type neurons in the compressed DRG. (A) Time histogram showing that local application of the I_{NaP} blocker riluzole reduces the basal firing rate of an A-type fiber in a dose-dependent manner (n = 6; P<0.05). (B) Percent inhibition of spontaneous activity in A-type fibers with respect to the concentration of locally-applied riluzole (μM; n = 6; *P<0.05, **P<0.01, ***P<0.001). (C) Time histogram showing the suppression of spontaneous activity induced by riluzole (100 μM) in an A-type afferent fiber from a compressed DRG. Expanded traces in right panel show firing patterns before (a) and during (b) the drug application.
doi:10.1371/journal.pone.0018681.g002

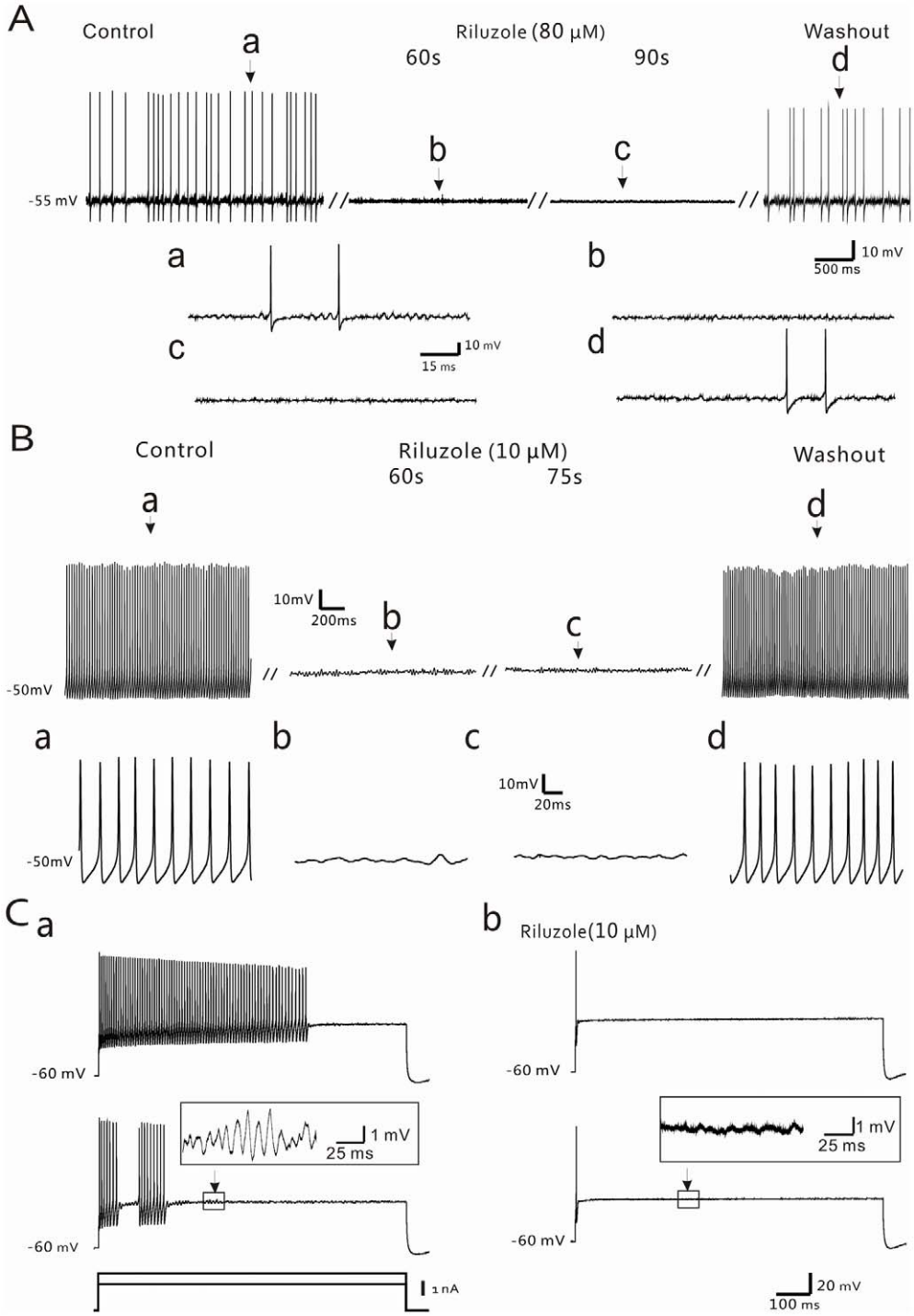

Figure 3. Effects of riluzole on the spontaneous activity and SMPOs of A-type neurons in the compressed DRG. (A) Intracellular sharp electrode recordings from an A-type DRG neuron *in vivo*, showing spontaneous activity and SMPOs under control conditions (a), after local application of riluzole (80 μM; b,c), and during washout (d). The spikes have been truncated. Inserted segments (a–d, lower panel) are expansions of the original traces at the times indicated and show details of the spikes and SMPOs. (B) Whole-cell patch recordings from an A-type DRG neuron *in vitro*. Spontaneous activity (a) was significantly inhibited in the presence of riluzole (10 μM; b,c) and restored after washout (d). The spikes have been truncated. Inserted segments (a–d, lower panel) are expansions of the original traces at the times indicated. (C) Whole-cell patch recordings from an A-type DRG neuron *in vitro*. (a) The cell responded to depolarizing current pulses of 1.7 nA (upper panel) and 2.4 nA (lower panel) with repetitive firing and SMPOs (insertion). (b) In the presence of 10 μM riluzole (upper panel), both the repetitive firing and SMPOs (insertion) induced by depolarization were abolished; however, a single action potential was still evoked immediately after application of the current pulse.
doi:10.1371/journal.pone.0018681.g003

application. It is interesting to note that although riluzole largely abolished the evoked SMPOs and the repetitive firing, these DRG neurons still responded to the same depolarizing current pulses with a single action potential at the initial phase of the current pulse, indicating that these cells are still capable of generating action potentials in the presence of riluzole (Fig. 3C). In all the neurons tested, the SMPOs and repetitive firing were largely recovered after riluzole washout.

4. Increased I_{NaP} in injured A-type DRG neurons

Using whole-cell patch-clamp methods, 114 large- and medium-sized neurons (≥35 μm in diameter) were recorded in *in vitro* DRG preparations taken from CCD animals. These neurons had a stable resting potential of −55.7±0.9 mV (n = 80), a membrane resistance of 89.6±5.3 MΩ (n = 80), and a membrane capacitance of 92.4±3.3 pF (n = 80).

In these experiments, the glass recording pipettes were filled with a Cs^+-based internal solution, while K^+ and Ca^{2+} channel blockers were added to the bath. Under a holding potential of −60 mV, I_{NaP} was recorded in normal DRG neurons by applying a 3 s depolarization ramp current from −80 to 0 mV [30]. The inward sodium current was induced at potentials of −60 to −50 mV, reached a peak at −35 mV, returned to control levels at −20 mV (Fig. 4A), and was sensitive to a low dose of TTX (100 nM, not shown). In injured A-type DRG neurons, the average current density of I_{NaP} was also significantly increased (CCD group: 2.8±0.3 pA/pF, control group: 1.6±0.3 pA/pF, non-paired t-test, $P<0.05$; Fig. 4A–4C). The activation curves of I_{NaP} in control and compressed DRG neurons were both fit with a Boltzmann distribution equation; the differences were not statistically significant (Fig. 4D).

5. Selective inhibitory effect of riluzole on I_{NaP} in injured A-type DRG neurons

The average current peak of I_{NaP} in injured A-type DRG neurons was 249.1±48.3 pA or 248.4±47.9 pA (n = 4) in the absence or presence of DMSO (0.1%), respectively, a difference which is not statistically significant (paired t-test, $P>0.05$; Fig. 4E&4F). Riluzole significantly inhibited the I_{NaP} of injured A-type DRG neurons in a dose-dependent manner. At doses as low as 2 μM, the drug clearly reduced the peak value of I_{NaP} by ~40% (n = 5, non-paired t-test, $P<0.05$; Fig. 5A), and the IC_{50} for riluzole inhibition of the I_{NaP} was 4.1 μM (n = 5; Fig. 5B).

To determine the specificity of this riluzole-induced inhibition in injured A-type DRG neurons, we next examined the effects of the drug on the TTX-sensitive transient sodium current (I_{NaT}). In whole-cell recordings performed under voltage-clamp, I_{NaT} was evoked by depolarization voltage steps (Fig. 5C). Riluzole was then bath-applied at 10, 200 and 500 μM, and the percent inhibition of the I_{NaT} peak amplitude in each neuron was plotted against the different voltage steps (Fig. 5D). The inhibition of I_{NaT} at 200 and 500 μM riluzole was 58.9±6.5% (n = 4, paired t-test, $P<0.05$) and 82.0±1.7% (n = 3, paired t-test, $P<0.001$), respectively.

Discussion

The primary finding of the present study is that a local application of the I_{NaP} blocker riluzole to the DRG selectively reduces the I_{NaP} and I_{NaP}-associated SMPOs of injured DRG neurons in the CCD animal model of neuropathic pain. The I_{NaP} is enhanced in medium- and large-sized DRG neurons of the compressed DRG.. Our data shows for the first time that the I_{NaP} and I_{NaP}-associated SMPOs of injured DRG neurons are important to the spontaneous activity of primary afferents in neuropathic pain states. Hence, the blockade of I_{NaP} in DRG neurons may play an anti-nociceptive role at the primary afferent level.

1. Spontaneous activity in neuropathic pain states

In our animal model, a chronic and steady compression is ipsilaterally applied to the DRG in rats (CCD model), causing the animals to show behaviors typical of mechanical allodynia ipisilaterally [24]. Ectopic spontaneous activity plays an important role in maintaining central sensitization and neuropathic pain. Moreover, the level of ectopic discharge is generally well correlated with the degree of pain behavior in neuropathic animals [31]. Our *in vivo* experiment demonstrate that the spontaneous activity of large diameter primary afferent fibers is inhibited by the I_{NaP} blocker riluzole in a dose-dependent manner and is completely abolished at a concentration of 500 μM. This concentration of riluzole was slightly higher than that of the riluzole used in our *in vitro* whole-cell patch-clamp experienments of the present study, due to the rapid circulation of blood within the DRG *in vivo*. These results indicate that the I_{NaP} blocker riluzole inhibits the spontaneous activity of compressed type-A DRG neurons, and hence reduces pathological pain signals originating in the periphery.

2. SMPOs in A-type DRG neurons

Previous work has shown that low levels of TTX also suppress SMPOs and abolish ectopic spontaneous activity in injured DRG neurons [32,33,34], indicating that SMPOs of injured DRG neurons are essential to the generation of abnormal spontaneous activity and pain behaviors. The fact that peripheral receptors and large parts of the axons were removed in our preparations suggests that SMPOs must be generated in the soma or in proximal segments of DRG cell axons. Hence, pathological hyperexcitability may originate not only at receptors in the skin but also in the somatic region of primary afferent neurons. Our recent work has shown that analgesic drugs such as gabapentin and lidocaine have inhibitory effects similar to those of riluzole on I_{NaP} [22,23]. The results reported here further demonstrate that I_{NaP} plays an important role in the generation of SMPOs that occur in injured A-type DRG neurons after compression of the DRG. In the rat trigeminal mesencephalic nuclei, I_{NaP} is responsible for the enhancement of SMPOs and also participates in the generation of bursting in central neurons [19]. Taken together, these studies strongly suggest that injury and inflammation may cause large- and medium-sized DRG neurons to increase a TTX-sensitive I_{NaP} and its associated SMPOs. The latter may in turn facilitate the generation of ectopic spontaneous activity, an important basis for pathological pain signals in the periphery under neuropathic pain states. Using sharp electrode recordings *in vivo* and whole-cell patch-clamp recordings *in vitro*, we observed sine wave-like SMPOs in DRG neurons. Moreover, although repetitive firing and SMPOs were abolished by riluzole, DRG neurons still responded to intracellular current injection with a single full-sized spike, demonstrating that they are still capable of firing action potentials under riluzole.

3. I_{NaP} in A-type DRG neurons

The vast majority of pain studies at the peripheral level have focused on small DRG neurons (<25 μm in diameter) and their fibers. However, in cases of allodynia the non-nociceptive stimuli associated with these cells become nociceptive, and almost any type of stimulus may cause pain. It is a reasonable hypothesis that medium- and large-sized primary afferent fibers and their DRG neurons are responsible for allodynia [35,36]. The present study

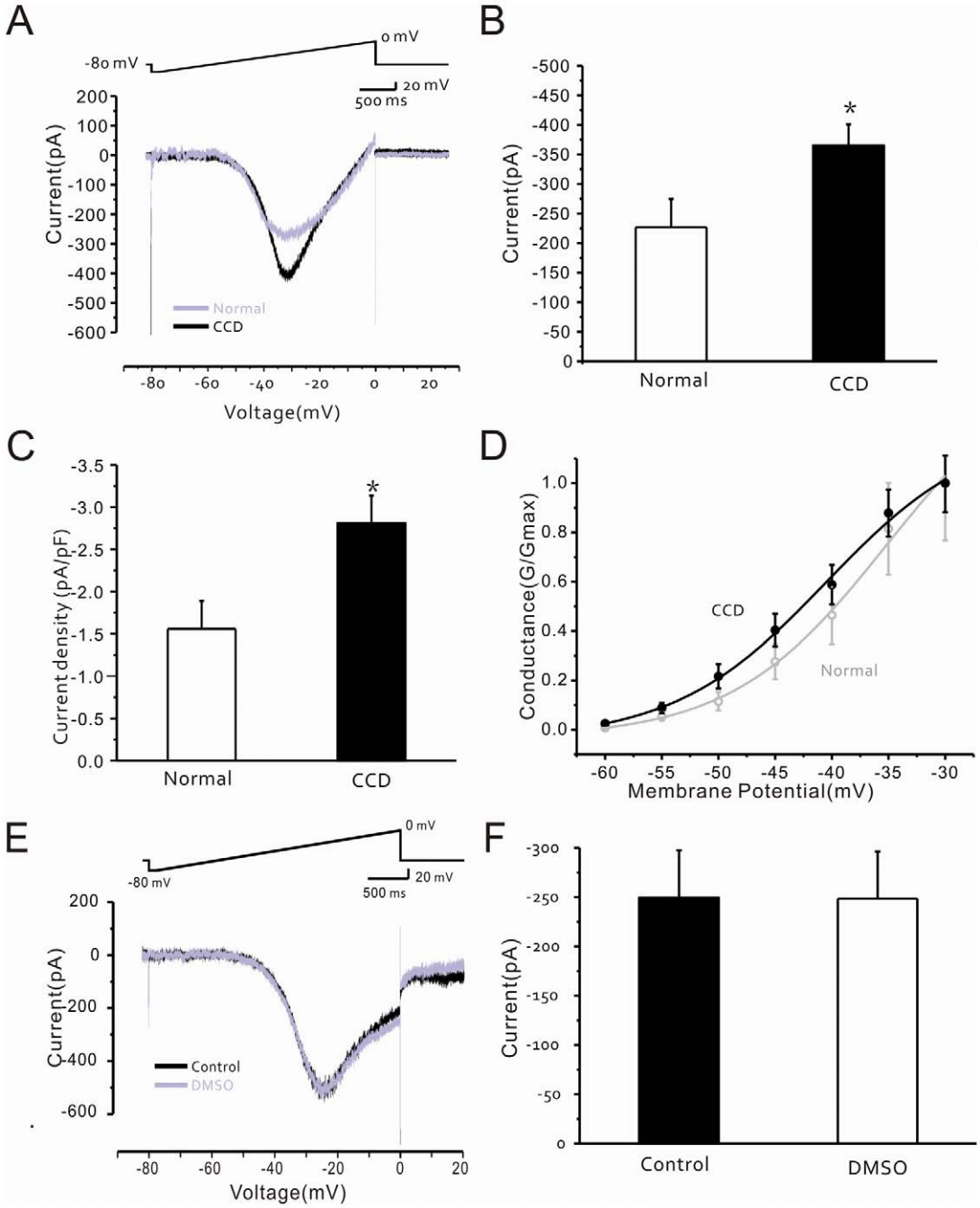

Figure 4. Enhanced I_{NaP} in A-type neurons of the compressed DRG. (A) Traces of I_{NaP} in A-type neurons from control (normal; grey line) and compressed (CCD, solid line) DRGs (bottom) as induced by increasing applied voltage (top). (B) Bar graph showing that the average peak I_{NaP} is significantly greater in neurons recorded from compressed DRGs (CCD; n = 31) compared to the average peak value from control group recordings (normal; n = 26; *P<0.05). (C) Bar graph showing that average peak I_{NaP} current density is significantly greater in compressed DRG neurons (n = 31) compared to the average peak value from control group recordings (n = 26; *P<0.05). (D) Steady state activation curves for I_{NaP} conductance with respect to voltage in control and compressed DRG neurons as fit with a Boltzmann distribution equation. The differences are not statistically significant. (E) Traces of I_{NaP} in a compressed DRG neuron in the absence (control, solid line) and presence (DMSO, grey line) of 0.1% DMSO (bottom) as induced by increasing applied voltage (top). (F) Bar graph showing that average peak I_{NaP} in compressed DRG neurons (n = 7) in the presence of 0.1% DMSO is not significantly different from the average peak I_{NaP} in the absence of DMSO (control, filled; n = 7; P>0.05).
doi:10.1371/journal.pone.0018681.g004

has focused on these neurons and their fibers in a CCG model to further characterize allodynia's cellular mechanisms.

I_{NaP} is a TTX-sensitive current that is activated in the subthreshold voltage range and is slowly inactivating. Such dynamics enable neurons to amplify their responses to synaptic inputs, thereby driving them to spiking or repetitive firing [9,11]. To measure I_{NaP} directly, we injected ramp current into the recorded cells while isolating the I_{NaP} by adding the non-selective K^+ channel blocker cesium to the internal solution and the non-selective Ca^{2+} channel blocker cadmium to the bath [30]. Our

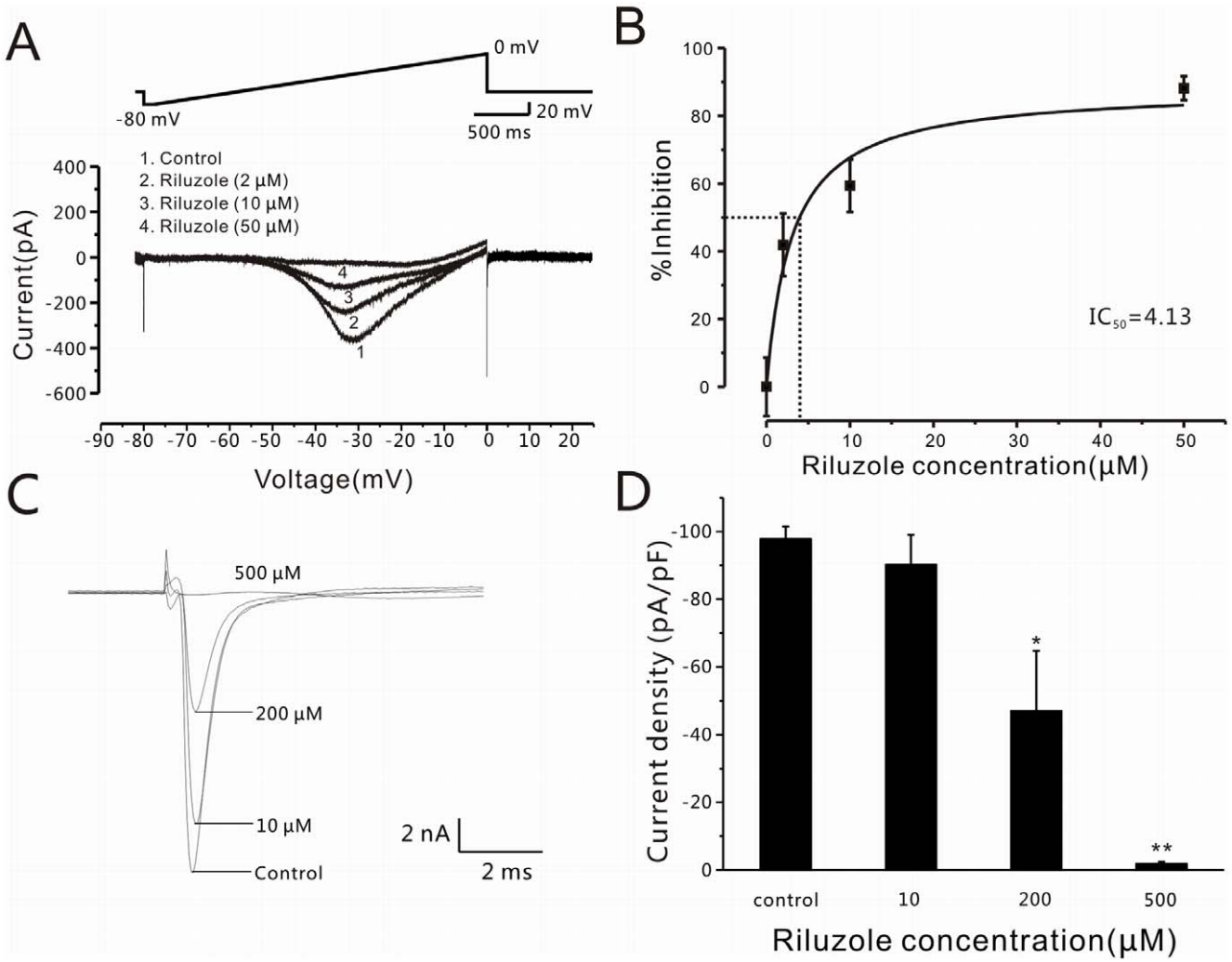

Figure 5. Effects of riluzole on I_{NaP} and I_{NaT} in A-type neurons of the compressed DRG. (A) Traces of I_{NaP} (bottom) induced by increasing applied voltage (top) in a compressed DRG neuron in the absence (control) and presence of riluzole (2, 10, 50 μM). (B) Dose-inhibition curve showing effect of locally applied riluzole on I_{NaP} in compressed DRG neurons (n = 5; IC_{50} = 4.3 μM). (C) I_{NaT} traces in a DRG neuron evoked by applied depolarization (−20 mV) under control conditions and in the presence of riluzole (10, 200, 500 μM). (D) Bar graph showing that average peak I_{NaT} current density (pA/pF) in the presence of riluzole (10, 200, 500 μM) is significantly decreased in neurons recorded from compressed DRGs (*P<0.05, **P<0.01).

doi:10.1371/journal.pone.0018681.g005

results show that I_{NaP} is indeed present in normal A-type DRG neurons and is blocked by the presence of a low concentration of TTX (100 nM). Moreover, after induction of the ganglion compression characteristic of the CCD model, I_{NaP} was significantly increased in A-type DRG neurons. I_{NaP} activation curves for compressed DRG neurons were not significantly different from those of the control group. These results suggest that increased I_{NaP} contributes to the hyperexcitability of injured A-type DRG neurons.

There is evidence that under experimental pain conditions, at least two types of Na^+ channels, $Na_v1.7$ and $Na_v1.8$, are upregulated and downregulated concurrently with corresponding effects on TTX-sensitive and TTX-insensitive currents [37]. The sodium channel $Na_v1.7$ is expressed predominantly in DRG and sympathetic ganglion neurons [38,39,40,41], specifically in most functionally-identified DRG nociceptive or small neurons [42]. This channel has been proposed as a molecular gatekeeper of pain detection at peripheral nociceptors [43]. $Na_v1.7$ is slowly inactivated with dynamics similar to those of I_{NaP} [44]. The expression of $Na_v1.7$ in large- and medium-sized DRG cells, in addition to its upregulation concurrent with changes in I_{NaP}, have been observed in a model of diabetic neuropathy [45]. There is also evidence that increased I_{NaP} determines cortical hyperexcitability in a genetic model of amyotrophic lateral sclerosis [11].

4. Potential anti-nociceptive effects of I_{NaP} blocker riluzole

Animal studies have shown that riluzole reduces the development of mechanical and cold hyperactivities in a neuropathic pain model through its pronounced suppression of glutamate and aspartate levels in the spinal dorsal horn [46]. Riluzole also attenuates formalin-induced flinching behaviors that follow from its blocking effects on sodium channels, although a specific site of this action has not been demonstrated [47]. In the rat, local injection of riluzole into the ventral posterolateral thalamic nuclei was found to reduce carrageenan-induced mechanical hyperalge-

sia due to a decrease in glutamate release [48]. In addition, riluzole was reported to induce anti-nociceptive effects along with a general anesthetic state, probably by blocking glutamatergic neurotransmission [49]. However, clinical research has shown that oral administration of riluzole does not affect thermal and mechanical hyperalgesia in patients with inflammatory pain [50] or alleviate allodynia and mechanical hyperalgesia in neuropathic pain patients [51].

These controversial effects of riluzole in clinical application and animal research call for simplified model systems to explore its basic mechanisms at cellular and molecular levels. To avoid the complexity of riluzole's effects on the CNS, we have systematically investigated its effects on DRG neurons as representing the first stage of the peripheral pain sensory system. We have shown that riluzole selectively inhibits the I_{NaP} of injured A-type DRG neurons, thereby suppressing their SMPOs and ectopic spotaneous activity. Those results suggest that the I_{NaP} of DRG neurons can be a potential target for analgesia at the peripheral level.

Our results indicating that riluzole may excert an anti-allodynia effect in the DRG after nerve injury are also consistent with reports that riluzole decreases the development of mechanical allodynia in a rat model of neuropathic pain [46] and that the drug attenuates nociceptive responses in a formalin-induced inflammatory model [47]. Clinically, however, riluzole does not affect thermal hyperalgesia in the inflammatory pain induced by heat stimuli [50]. These results strongly suggest that riluzole selectively reduces mechanical allodynia under neuropathic pain states, but is not as effective in treating other types of pain that are conveyed via thin afferent fibers. Compared with the anti-convulsant agents gabapentin and lamotrigine, lower doses of riluzole were more effective in relieving mechanical hypersensitivity. The effects of the drug were also long-lasting, extending up to 12 days after systematic administration [46]. Apparently, riluzole is much more efficient than these other agents in reducing mechanical hypersensitivity under conditions of neuropathic pain. The discrepancy of its clinical ineffectiveness may be due to the use of insufficient doses of the drug at local sites. Our recent work showing that I_{NaP} is suppressed by gabapentin and low doses of lidocaine in compressed DRG neurons [22,23], as well as the inhibitory effects of riluzole in the same CCG model shown here, indicate that the I_{NaP} of injured DRG neurons remains a potential target for analgesia at the peripheral level.

From a clinical point of view, most pain symptoms in peripheral neuropathy are of peripheral origin [52]. The gateway function of the DRG suggests that the I_{NaP} of DRG neurons could be a potential target in treating patients with peripheral pain symptoms. Our results demonstrate that local application of I_{NaP} blocker riluzole within the DRG could be specific and effective as a peripherally-acting analgesic agent that does not penetrate the blood-brain barrier and is therefore free of central nervous system side effects [53].

Acknowledgments

We thank Drs. Victor Z. Han and Jerry Magnus for their comments on the manuscript.

Author Contributions

Conceived and designed the experiments: S-JH HX. Performed the experiments: R-GX D-WZ X-JZ YS FK. Analyzed the data: R-GX D-WZ X-JZ YS Y-BX. Contributed reagents/materials/analysis tools: S-WY J-LX HD. Wrote the paper: HX S-JH.

References

1. Crill WE (1996) Persistent sodium current in mammalian central neurons. Annu Rev Physiol 58: 349–362.
2. Jahnsen H, Llinas R (1984) Ionic basis for the electro-responsiveness and oscillatory properties of guinea-pig thalamic neurones in vitro. J Physiol 349: 227–247.
3. Wu N, Enomoto A, Tanaka S, Hsiao CF, Nykamp DQ, et al. (2005) Persistent sodium currents in mesencephalic v neurons participate in burst generation and control of membrane excitability. J Neurophysiol 93: 2710–2722.
4. Zeng J, Powers RK, Newkirk G, Yonkers M, Binder MD (2005) Contribution of persistent sodium currents to spike-frequency adaptation in rat hypoglossal motoneurons. J Neurophysiol 93: 1035–1041.
5. Stafstrom CE (2007) Persistent sodium current and its role in epilepsy. Epilepsy Curr 7: 15–22.
6. Urbani A, Belluzzi O (2000) Riluzole inhibits the persistent sodium current in mammalian CNS neurons. Eur J Neurosci 12: 3567–3574.
7. Do MT, Bean BP (2003) Subthreshold sodium currents and pacemaking of subthalamic neurons: modulation by slow inactivation. Neuron 39: 109–120.
8. Vervaeke K, Hu H, Graham LJ, Storm JF (2006) Contrasting effects of the persistent Na+ current on neuronal excitability and spike timing. Neuron 49: 257–270.
9. Tazerart S, Vinay L, Brocard F (2008) The persistent sodium current generates pacemaker activities in the central pattern generator for locomotion and regulates the locomotor rhythm. J Neurosci 28: 8577–8589.
10. Yue C, Remy S, Su H, Beck H, Yaari Y (2005) Proximal persistent Na+ channels drive spike afterdepolarizations and associated bursting in adult CA1 pyramidal cells. J Neurosci 25: 9704–9720.
11. Pieri M, Carunchio I, Curcio L, Mercuri NB, Zona C (2009) Increased persistent sodium current determines cortical hyperexcitability in a genetic model of amyotrophic lateral sclerosis. Exp Neurol 215: 368–379.
12. Lampert A, Hains BC, Waxman SG (2006) Upregulation of persistent and ramp sodium current in dorsal horn neurons after spinal cord injury. Exp Brain Res 174: 660–666.
13. Del NC, Morgado-Valle C, Hayes JA, Mackay DD, Pace RW, et al. (2005) Sodium and calcium current-mediated pacemaker neurons and respiratory rhythm generation. J Neurosci 25: 446–453.
14. Harvey PJ, Li Y, Li X, Bennett DJ (2006) Persistent sodium currents and repetitive firing in motoneurons of the sacrocaudal spinal cord of adult rats. J Neurophysiol 96: 1141–1157.
15. Lamanauskas N, Nistri A (2008) Riluzole blocks persistent Na+ and Ca2+ currents and modulates release of glutamate via presynaptic NMDA receptors on neonatal rat hypoglossal motoneurons in vitro. Eur J Neurosci 27: 2501–2514.
16. Miles GB, Dai Y, Brownstone RM (2005) Mechanisms underlying the early phase of spike frequency adaptation in mouse spinal motoneurones. J Physiol 566: 519–532.
17. Theiss RD, Kuo JJ, Heckman CJ (2007) Persistent inward currents in rat ventral horn neurones. J Physiol 580: 507–522.
18. Kononenko NI, Shao LR, Dudek FE (2004) Riluzole-sensitive slowly inactivating sodium current in rat suprachiasmatic nucleus neurons. J Neurophysiol 91: 710–718.
19. Wu N, Hsiao CF, Chandler SH (2001) Membrane resonance and subthreshold membrane oscillations in mesencephalic V neurons: participants in burst generation. J Neurosci 21: 3729–3739.
20. Wokke J (1996) Riluzole. Lancet 348: 795–799.
21. Song JH, Huang CS, Nagata K, Yeh JZ, Narahashi T (1997) Differential action of riluzole on tetrodotoxin-sensitive and tetrodotoxin-resistant sodium channels. J Pharmacol Exp Ther 282: 707–714.
22. Dong H, Fan YH, Wang YY, Wang WT, Hu SJ (2008) Lidocaine suppresses subthreshold oscillations by inhibiting persistent Na(+) current in injured dorsal root ganglion neurons. Physiol Res 57: 639–645.
23. Yang RH, Wang WT, Chen JY, Xie RG, Hu SJ (2009) Gabapentin selectively reduces persistent sodium current in injured type-A dorsal root ganglion neurons. Pain 143: 48–55.
24. Hu SJ, Xing JL (1998) An experimental model for chronic compression of dorsal root ganglion produced by intervertebral foramen stenosis in the rat. Pain 77: 15–23.
25. Song XJ, Hu SJ, Greenquist KW, Zhang JM, LaMotte RH (1999) Mechanical and thermal hyperalgesia and ectopic neuronal discharge after chronic compression of dorsal root ganglia. J Neurophysiol 82: 3347–3358.
26. Chaplan SR, Bach FW, Pogrel JW, Chung JM, Yaksh TL (1994) Quantitative assessment of tactile allodynia in the rat paw. J Neurosci Methods 53: 55–63.
27. Dong XW, Jia Y, Lu SX, Zhou X, Cohen-Williams M, et al. (2008) The antipsychotic drug, fluphenazine, effectively reverses mechanical allodynia in rat models of neuropathic pain. Psychopharmacology (Berl) 195: 559–568.
28. Hu SJ, Yang HJ, Jian Z, Long KP, Duan YB, et al. (2000) Adrenergic sensitivity of neurons with non-periodic firing activity in rat injured dorsal root ganglion. Neuroscience 101: 689–698.
29. Xie Y, Zhang J, Petersen M, LaMotte RH (1995) Functional changes in dorsal root ganglion cells after chronic nerve constriction in the rat. J Neurophysiol 73: 1811–1820.

30. Reboreda A, Sanchez E, Romero M, Lamas JA (2003) Intrinsic spontaneous activity and subthreshold oscillations in neurones of the rat dorsal column nuclei in culture. J Physiol 551: 191–205.
31. Sheen K, Chung JM (1993) Signs of neuropathic pain depend on signals from injured nerve fibers in a rat model. Brain Res 610: 62–68.
32. Amir R, Michaelis M, Devor M (1999) Membrane potential oscillations in dorsal root ganglion neurons: role in normal electrogenesis and neuropathic pain. J Neurosci 19: 8589–8596.
33. Liu CN, Michaelis M, Amir R, Devor M (2000) Spinal nerve injury enhances subthreshold membrane potential oscillations in DRG neurons: relation to neuropathic pain. J Neurophysiol 84: 205–215.
34. Xing JL, Hu SJ, Long KP (2001) Subthreshold membrane potential oscillations of type A neurons in injured DRG. Brain Res 901: 128–136.
35. Song XJ, Wang ZB, Gan Q, Walters ET (2006) cAMP and cGMP contribute to sensory neuron hyperexcitability and hyperalgesia in rats with dorsal root ganglia compression. J Neurophysiol 95: 479–492.
36. Liu CN, Wall PD, Ben-Dor E, Michaelis M, Amir R, et al. (2000) Tactile allodynia in the absence of C-fiber activation: altered firing properties of DRG neurons following spinal nerve injury. Pain 85: 503–521.
37. Rush AM, Cummins TR, Waxman SG (2007) Multiple sodium channels and their roles in electrogenesis within dorsal root ganglion neurons. J Physiol 579: 1–14.
38. Black JA, Dib-Hajj S, McNabola K, Jeste S, Rizzo MA, et al. (1996) Spinal sensory neurons express multiple sodium channel alpha-subunit mRNAs. Brain Res Mol Brain Res 43: 117–131.
39. Sangameswaran L, Fish LM, Koch BD, Rabert DK, Delgado SG, et al. (1997) A novel tetrodotoxin-sensitive, voltage-gated sodium channel expressed in rat and human dorsal root ganglia. J Biol Chem 272: 14805–14809.
40. Toledo-Aral JJ, Moss BL, He ZJ, Koszowski AG, Whisenand T, et al. (1997) Identification of PN1, a predominant voltage-dependent sodium channel expressed principally in peripheral neurons. Proc Natl Acad Sci U S A 94: 1527–1532.
41. Waxman SG (2007) Channel, neuronal and clinical function in sodium channelopathies: from genotype to phenotype. Nat Neurosci 10: 405–409.
42. Djouhri L, Newton R, Levinson SR, Berry CM, Carruthers B, et al. (2003) Sensory and electrophysiological properties of guinea-pig sensory neurones expressing Nav 1.7 (PN1) Na+ channel alpha subunit protein. J Physiol 546: 565–576.
43. Drenth JP, Waxman SG (2007) Mutations in sodium-channel gene SCN9A cause a spectrum of human genetic pain disorders. J Clin Invest 117: 3603–3609.
44. Cummins TR, Howe JR, Waxman SG (1998) Slow closed-state inactivation: a novel mechanism underlying ramp currents in cells expressing the hNE/PN1 sodium channel. J Neurosci 18: 9607–9619.
45. Hong S, Morrow TJ, Paulson PE, Isom LL, Wiley JW (2004) Early painful diabetic neuropathy is associated with differential changes in tetrodotoxin-sensitive and -resistant sodium channels in dorsal root ganglion neurons in the rat. J Biol Chem 279: 29341–29350.
46. Coderre TJ, Kumar N, Lefebvre CD, Yu JS (2007) A comparison of the glutamate release inhibition and anti-allodynic effects of gabapentin, lamotrigine, and riluzole in a model of neuropathic pain. J Neurochem 100: 1289–1299.
47. Munro G, Erichsen HK, Mirza NR (2007) Pharmacological comparison of anticonvulsant drugs in animal models of persistent pain and anxiety. Neuropharmacology 53: 609–618.
48. Abarca C, Silva E, Sepulveda MJ, Oliva P, Contreras E (2000) Neurochemical changes after morphine, dizocilpine or riluzole in the ventral posterolateral thalamic nuclei of rats with hyperalgesia. Eur J Pharmacol 403: 67–74.
49. Irifune M, Kikuchi N, Saida T, Takarada T, Shimizu Y, et al. (2007) Riluzole, a glutamate release inhibitor, induces loss of righting reflex, antinociception, and immobility in response to noxious stimulation in mice. Anesth Analg 104: 1415–1421.
50. Hammer NA, Lilleso J, Pedersen JL, Kehlet H (1999) Effect of riluzole on acute pain and hyperalgesia in humans. Br J Anaesth 82: 718–722.
51. Galer BS, Twilling LL, Harle J, Cluff RS, Friedman E, et al. (2000) Lack of efficacy of riluzole in the treatment of peripheral neuropathic pain conditions. Neurology 55: 971–975.
52. Baron R (2009) Neuropathic pain: a clinical perspective. Handb Exp Pharmacol. pp 3–30.
53. Devor M (2009) Ectopic discharge in Abeta afferents as a source of neuropathic pain. Exp Brain Res 196: 115–128.